Contribution from the Department of Chemistry, Stanford University, Stanford, California 94305, and Division of Chemistry and Chemical Engineering, California Institute of Technology, Pasadena, California 91125

Preparation and Characterization of a Bis(pentaammineosmium(II)) Pyrene Complex

Tai Hasegawa,† Mikiya Sekine,† William P. Schaefer,‡ and Henry Taube*,†

Received July 14, 1989

It is known that addition of a second pentaammineosmium(II) ion to a pentaammineosmium(II) naphthalene complex takes place preferentially on the ring already coordinated; this work shows that when pyrene is the ligand, separate rings are occupied by the metal ions. The structure of $[(Os(NH_3)_5)_2(\mu\text{-pyrene})](O_3SCF_3)_4 \cdot 4(CH_3)_2CO$, a salt of the resulting binuclear cation, has been determined by X-ray diffraction. It crystallizes in the monoclinic system, in space group $P2_1/c$, with a = 11.475 (2) Å, b = 17.001 (5) Å, c = 15.846 (4) Å, β = 109.55 (2)°, and V = 2193.1 (13) Å^3; Z = 2. The electrochemical behavior of the cation, as determined by cyclic voltammetry, shows that the communication between the metal centers in the mixed-valence forms is weak. These results are in accord with expectations based on qualitative ideas on the effects arising from bond conjugation.

Introduction

Recently η^2-coordinated metal arene complexes have attracted special attention because of their possible intervention as intermediates in C-H activation.[1] With the advent[2a] of such robust species, other kinds of reactivity for the bound aromatic ligand are being explored.[2a-d] Of greatest interest for present purposes is the capacity of a ligand bound in η^2 fashion to $Os(NH_3)_5^{2+}$ to become attached to a second metal moiety, a capacity demonstrated even for the single-ring aromatic benzene. In fact, for benzene, the affinity of the ring for $Os(NH_3)_5^{2+}$ is increased by the addition of the first, an outcome which appears reasonable when account is taken of the fact that, upon addition of the first metal moiety, much of the "aromatic" stabilization of the ring is lost.

The bis(pentaammineosmium(II)) complex has an additional element of interest in that a mixed-valence molecule is easily generated by $1e^-$ oxidation.[2a] This offers the prospect of exploring a whole family of mixed-valence molecules based on fused-ring systems for the purpose of learning how the organic bridging group mediates in electron delocalization between two attached metal centers. But, in the extension of an investigation of this kind to naphthalene[3] and to anthracene,[4] it was found that the second $Os(NH_3)_5^{2+}$ attaches to the same ring as the first, a disappointing outcome for the declared purpose, though not a surprising one when the loss of aromatic stabilization by η^2-bond formation is taken into account.

The same kind of consideration led to the choice of pyrene as the organic ligand because here there appeared to be a good prospect that a bis(pentaammineosmium(II)) complex could be prepared in which the two metals occupy different rings. This has proven to be the case, and we herein report our work in characterizing the resulting complex.

Experimental Section

Syntheses. Dimethoxyethane (DME) was purified by vacuum distillation over NaK. *N,N*-Dimethylacetamide (DMA) was dried over BaO and then refluxed for 24 h and distilled from triphenylsilyl chloride. The resulting material was then refluxed with CaH_2 for 24 h and distilled to remove traces of HCl. Mg turnings were cleaned in a DME solution of iodine for 1 h, followed by copious washing with DMA, acetone, and Et_2O. NaOTf (OTf = CF_3SO_3) was recrystallized from acetone and ether. All other reagents were used as supplied.

All solvents were deoxygenated by purging with argon, and reactions were carried out under an argon atmosphere in a Vacuum Atmospheres Corp. glovebox.

$[Os(NH_3)_5(pyrene)](OTf)_2$ (1). $[Os(NH_3)_5(OTf)](OTf)_2$[5] (200 mg) dispersed in DME (10 mL) was dissolved completely by the addition of several drops of DMA (ca. 0.5 mL). To this solution were added pyrene (1 g, ca. 18 equiv) and Mg turnings (1.5 g) to reduce Os(III) to Os(II). The solution changed from yellow to dark red. The reaction mixture was stirred, and after 45 min, Mg was removed by filtration. The filtrate was added slowly to CH_2Cl_2 (100 mL) to precipitate a yellow product, which was isolated by filtration and washed with 200 mL of ether. Yield: 93%.

Table I. Crystallographic Data for the Osmium-Pyrene Complex

$Os_2N_{10}C_{32}O_{16}S_4F_{12}H_{64}$	$P2_1/c$ (No. 14)
fw = 1581.56	T = 23 °C
a = 11.475 (2) Å	λ = 0.71073 Å
b = 17.011 (5) Å	ρ_{calc} = 2.395 g cm^{-3}
c = 15.846 (4) Å	μ = 48.66 cm^{-1}
β = 109.55 (2)°	transm coeff = 0.54-0.76
V = 2193.1 (13) Å^3	$R(F_o)$, for all $F_o > 0$: 0.065
Z = 2	

^{1}H NMR in acetone-d_6: 8.02 (H_e, 2 H, dd, J_{be} = 7.2 Hz, J_{de} = 1.0 Hz), 7.93 (H_d, 2 H, dd, J_{bd} = 7.2 Hz), 7.93 (H_c, 2 H, s), 7.76 (H_b, 2 H, t), 5.78 (H_a, 2 H, s), 4.94 (trans NH_3, 3 H, s), 3.38 (cis NH_3, 12 H, s).

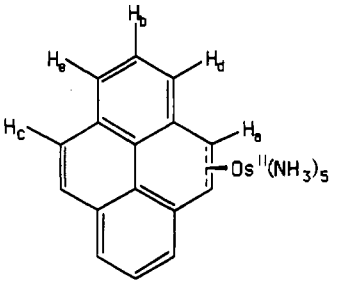

$[(Os(NH_3)_5)_2(pyrene)](OTf)_4 \cdot 4(CH_3)_2CO$ (2). $[Os(NH_3)_5(pyrene)](OTf)_2$ (75.0 mg, 9.67 × 10^{-5} mol) and $[Os(NH_3)_5(OTf)](OTf)_2$ (76.8 mg, 1.06 × 10^{-4} mol, 1.1 equiv) were dispersed in DME (5 mL) and dissolved by the addition of DMA (1 mL). Mg turnings (0.3 g) were added, and the mixture was stirred for 45 min. After the addition of another 0.3 g of Mg turnings, the mixture was stirred for another 45 min. The solution became cloudy and dark red. Excess Mg turnings were removed by filtration. The filtrate was added dropwise to 100 mL of CH_2Cl_2. The precipitate that had formed was filtered out and washed with ether. Yield: 78% based on **1** ($[Os(NH_3)_5(pyrene)](OTf)_2$).

Single crystals of $[(Os(NH_3)_5)_2(pyrene)](OTf)_4 \cdot 4(CH_3)_2CO$ were grown by the vapor diffusion method with acetone as the solvent and cyclohexane as the vapor.

^{1}H NMR in acetone-d_6: 7.68 (H_b, 4 H, d, J_{bc} = 7.2 Hz), 7.50 (H_c, 2 H, t), 5.53 (H_a, 4 H, s), 4.95 (trans NH_3, 6 H, s), 3.43 (cis NH_3, 24 H, s). ^{1}H NMR in acetone-d_6/DMSO-d_6 (9/1 w/w): 7.61 (H_b, 4 H,

† Stanford University.
‡ California Institute of Technology.

(1) (a) Chatt, J.; Davidson, J. M. *J. Chem. Soc.* **1965**, 843. (b) Jones, W. D.; Feher, F. J. *J. Am. Chem. Soc.* **1982**, *104*, 4240. (c) Sweet, J. R.; Graham, W. A. G. *Organometallics* **1983**, *2*, 135. (d) Sweet, J. R.; Graham, W. A. G. *J. Am. Chem. Soc.* **1983**, *105*, 305. (e) Jones, W. D.; Feher, F. J. *J. Am. Chem. Soc.* **1984**, *106*, 1650. (f) Cordone, R.; Taube, H. *J. Am. Chem. Soc.* **1987**, *109*, 8101.
(2) (a) Harman, W. D.; Taube, H. *J. Am. Chem. Soc.* **1987**, *109*, 1883. (b) Harman, W. D.; Sekine, M.; Taube, H. *J. Am. Chem. Soc.* **1988**, *110*, 2439. (c) Harman, W. D.; Taube, H. *J. Am. Chem. Soc.* **1988**, *110*, 7555. (d) Harman, W. D.; Taube, H. *J. Am. Chem. Soc.* **1988**, *110*, 7906. (e) Neithamer, D. R.; Parkanyi, L.; Mitchell, J. F.; Wolczanski, P. T. *J. Am. Chem. Soc.* **1988**, *110*, 4421.
(3) Harman, W. D.; Taube, H. *J. Am. Chem. Soc.* **1988**, *110*, 7555.
(4) Hasegawa, T.; Sekine, M. Work in progress.
(5) Lay, P. A.; Magnuson, R. H.; Sen, J.; Taube, H. *J. Am. Chem. Soc.* **1982**, *104*, 7658.

0020-1669/91/1330-0449$02.50/0

Table II. Final Parameters for the Osmium–Pyrene Complex (x, y, z, and $U_{eq}{}^{a} \times 10^4$)

atom	x	y	z	U_{eq} or B, Å^2
Os	163 (0.5)	2146 (0.4)	397 (0.4)	425 (2)
N1	2169 (11)	2284 (8)	801 (8)	4.7 (3)[b]
N2	154 (10)	1599 (7)	−847 (8)	4.0 (3)[b]
N3	−1819 (10)	2375 (7)	−168 (8)	4.1 (3)[b]
N4	203 (10)	2769 (7)	1579 (7)	4.2 (3)[b]
N5	227 (10)	3272 (7)	−263 (8)	4.4 (3)[b]
C1	773 (12)	1108 (9)	1232 (9)	3.5 (3)[b]
C2	1373 (13)	506 (9)	842 (10)	3.8 (3)[b]
C3	2689 (14)	438 (10)	1142 (10)	4.5 (4)[b]
C4	3252 (15)	−74 (10)	718 (12)	5.2 (4)[b]
C5	671 (12)	−25 (9)	150 (10)	3.5 (3)[b]
C6	−2570 (14)	575 (9)	−10 (10)	4.4 (4)[b]
C7	−1264 (13)	552 (9)	248 (10)	3.8 (3)[b]
C8	−554 (13)	1154 (9)	932 (10)	4.3 (4)[b]
S1	7454 (4)	2482 (4)	2340 (4)	777 (18)
O1	8294 (12)	1936 (9)	2857 (9)	1284 (56)
O2	7452 (12)	2620 (11)	1459 (9)	1475 (68)
O3	7414 (16)	3186 (9)	2847 (10)	1447 (70)
C9	5885 (26)	2109 (19)	2182 (20)	9.7 (7)[b]
F1	5914 (14)	1828 (13)	2943 (12)	2237 (79)
F2	5844 (13)	1455 (10)	1643 (12)	1859 (69)
F3	5081 (10)	2585 (10)	1776 (12)	1860 (74)
S2	2938 (5)	2221 (6)	3697 (4)	1172 (26)
O4	1955 (17)	2496 (18)	3521 (13)	2554 (124)
O5	3211 (29)	1687 (11)	4618 (16)	2641 (115)
O6	3298 (19)	1718 (17)	3119 (15)	3148 (112)
C10	4356 (33)	2738 (22)	4295 (26)	12.2 (9)[b]
F4	4241 (31)	3179 (13)	3484 (21)	3575 (140)
F5	5231 (14)	2292 (14)	4483 (11)	2147 (82)
F6	3856 (24)	3276 (11)	4679 (15)	2730 (99)
O20	2025 (16)	978 (11)	6381 (12)	11.8 (5)[b]
O21	8396 (16)	858 (11)	5437 (12)	12.4 (5)[b]
C20	2741 (25)	528 (16)	6918 (19)	10.9 (8)[b]
C21	2418 (25)	196 (16)	7707 (19)	12.1 (8)[b]
C22	4020 (27)	457 (16)	6855 (18)	12.3 (8)[b]
C23	7899 (27)	501 (17)	5881 (20)	11.1 (8)[b]
C24	6517 (30)	459 (18)	5604 (20)	14.2 (10)[b]
C25	8641 (28)	108 (18)	6726 (22)	13.9 (10)[b]

[a] $U_{eq} = {}^1/_3\sum_i\sum_j[U_{ij}(a_i^*a_j^*)(\vec{a}_i\cdot\vec{a}_j)]$. [b] Isotropic displacement parameter, B.

d), 7.50 (H_c, 2 H, t), 5.30 (H_a, 4 H, s), 4.77 (trans NH_3, 6 H, s), 3.24 (cis NH_3, 12 H, s).

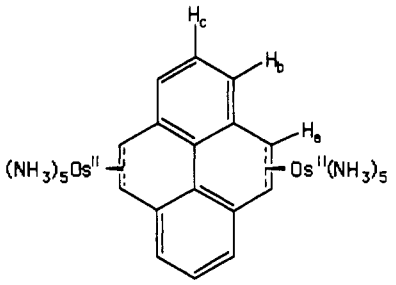

Structure Determination. A crystal of **2** was mounted in a capillary and centered on the diffractometer; unit cell dimensions plus the orientation matrix were calculated from the setting angles of 25 reflections with $18° < 2\theta < 24°$. Crystallographic data are given in Table I. $Os_2N_{10}C_{32}O_{16}S_4F_{12}H_{64}$ crystallizes in the monoclinic system, in space group $P2_1/c$, with $a = 11.475$ (2) Å, $b = 17.001$ (5) Å, $c = 15.846$ (4) Å, $\beta = 109.55$ (2)°, and $Z = 2$. A CAD-4 diffractometer was used; 6040 reflections were measured (2635 independent) and all were used in the refinement; 2471 reflections with $F_o^2 > 0$ were used to calculate R of 0.065 and 2039 with $F_o^2 > 3\sigma(F_o^2)$, giving R squares refinement. Two equivalent data sets were collected and merged to give the final set. The osmium atom position was found from a Patterson map, and the remainder of the atoms were located by successive structure factor–Fourier calculations. Atoms of the two independent anions were not sharply defined in the Fourier maps. Refinement was by least squares, with intermediate attempts to improve the results with difference Fourier maps. The osmium atom and the sulfur, oxygen, and fluorine atoms of the triflate anions were assigned anisotropic thermal parameters; other atoms were refined isotropically for reasons of economy. The two trifluoromethanesulfonate anions behaved poorly in the refinement, with unrealistic S–O and C–F distances. At convergence, structure factors were calculated by leaving one anion at a time out, and difference Fourier maps were calculated in the anion regions. These showed major peaks at the positions to which the atoms had refined, as well as eight or nine secondary peaks (~1–1.5 e Å^{-3}) scattered about. We could not derive a possible alternate location for an anion at either site, so we accepted the unsatisfactory result as refined. The final difference map has one peak of 1.5 e Å^{-3} and three holes of −1.20, −1.15, and −1.02 e Å^3; all other maxima and minima excursions are less than ±1 e Å^3. All large peaks are near the anion positions. Final parameters are listed in Table II.

Calculations were done with programs of the CRYM Crystallographic Computing System and ORTEP. Scattering factors and corrections for anomalous scattering were taken from a standard reference.[6] $R = \sum||F_o| - |F_c||/\sum F_o$, for only $F_o^2 > 0$, and goodness of fit = $[\sum w(F_o^2 - F_c^2)^2/(n - p)]^{1/2}$, where n is the number of data and p the number of parameters refined. The function minimized in least squares was $\sum w(F_o^2 - F_c^2)^2$, where $w = 1/\sigma^2(F_o^2)$. Variances of the individual reflections were assigned on the basis of counting statistics plus an additional term, $0.014I^2$. Variances of the merged reflections were assigned on the basis of counting statistics plus an additional term, $0.014I^2$. Variances of the merged reflections were determined by standard propagation of error plus another additional term, $0.014\langle I\rangle^2$. The absorption correction was done by Gaussian integration over an 8 × 8 × 8 grid. Transmission factors varied from 0.54 to 0.76. The secondary extinction parameter[7a] refined to 0.046 (13) × 10^{-6}.

Electrochemistry. Electrochemical experiments were performed under argon with a PAR Model 173 potentiostat driven by a PAR Model 175

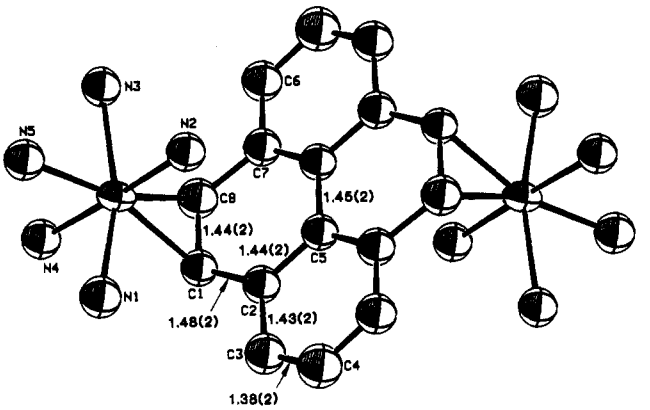

Figure 1. ORTEP drawing of the cation showing the numbering system and some selected distances. Thermal ellipsoids are drawn at the 50% probability level.

Table III. Selected Distances and Angles

	Distances (Å)		
Os–N1	2.186 (13)	C1–C8	1.44 (2)
Os–N2	2.175 (12)	C2–C3	1.43 (2)
Os–N3	2.183 (12)	C2–C5	1.44 (2)
Os–N4	2.140 (12)	C3–C4	1.38 (2)
Os–N5	2.195 (12)	C4–C6	1.42 (2)
Os–C1	2.175 (14)	C5–C5	1.45 (2)
Os–C8	2.169 (15)	C5–C7	1.40 (2)
Os–C1,8	2.050 (15)	C6–C7	1.42 (2)
C1–C2	1.48 (2)	C7–C8	1.51 (2)
	Angles (deg)		
N2–Os–N1	89.8 (5)	N5–Os–N4	89.4 (4)
N3–Os–N1	162.1 (5)	C1,8–Os–N4	87.1 (5)
N4–Os–N1	88.8 (5)	C1,8–Os–N5	176.5 (5)
N5–Os–N1	81.2 (5)	C8–C1–C2	119.3 (13)
C1,8–Os–N1	98.7 (5)	C3–C2–C1	120.3 (13)
N3–Os–N2	91.0 (4)	C5–C2–C1	122.1 (13)
N4–Os–N2	175.5 (4)	C5–C2–C3	117.6 (14)
N5–Os–N2	86.2 (4)	C4–C3–C2	120.2 (15)
C1,8–Os–N2	97.4 (5)	C6–C4–C3	122.6 (16)
N4–Os–N3	89.1 (4)	C5–C5–C2	118.3 (13)
N5–Os–N3	81.1 (4)	C7–C5–C2	120.9 (14)
C1,8–Os–N3	99.0 (5)	C7–C5–C5	120.8 (14)

(6) *International Tables for X-ray Crystallography*; Kynoch Press: Birmingham, U.K., 1974; Vol. IV, pp 71, 149.
(7) (a) Larson, E. C. *Acta Crystallogr.* **1967**, *23*, 664 (eq 3). (b) Harman, W. D. Ph.D. Thesis, Stanford University, 1987.

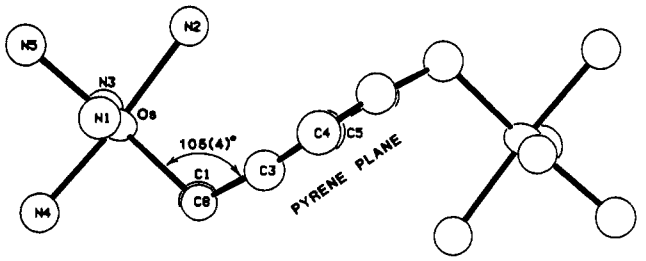

Figure 2. ORTEP drawing of the cation showing the osmium to C=C bonding. Thermal ellipsoids are drawn at the 50% probability level.

universal programmer. Cyclic voltammograms were recorded from +1.5 to −1.5 V (NHE) with a Pt^0 working electrode (5 mm^2), a Pt^0 counter electrode, and a reference cell consisting of an Au^0 button in a DME solution containing NaOTf separated from the main cell by a Vycor frit. The reference was calibrated with the ferrocene/ferrocenium couple (E^0 ≡ 0.55 V; NHE) kept in situ. The peak-to-peak separation for this couple varied in the range 60–120 mV depending on cell conditions for the cyclic voltammograms reported. The scan rate is 100 mV/s unless otherwise stated. All potentials are reported vs the normal hydrogen electrode.

Results

Structure Description. The pentaammineosmium fragments are π-bonded to the pyrene ligand in a trans fashion. Coordination about the osmium atom is distorted octahedral (taking the C=C group as one ligand) or distorted pentagonal bipyramidal (taking the two carbon atoms as separate ligands), with the ammine groups shifting to minimize nonbonded ligand–ligand interactions. The resultant geometry can be seen in Figure 1: N1 and N3 are displaced away from the pyrene, as is N2, while N4 is pushed somewhat toward it. Selected distances and angles are recorded in Table III. The nonbonded distances about osmium and the ligand–Os–ligand angles are listed in Table SII (supplementary material). Distances and angles in the pyrene ligand are as expected. The bonds C1–C2 and C7–C8 next to the carbon atoms bonded to osmium are longer (1.50 (2) Å) than the rest of the bonds, which average 1.42 (2) Å and range from 1.38 (2) (C3–C4) to 1.45 (2) Å (C5–C5′). There is no clear pattern of alternating single and double bonds, however. The trans osmium atoms are about 2 Å out of the plane of the pyrene ring, which is planar within ±0.08 Å. The angle between the pyrene plane and the Os–C1–C8 plane is 105 (4)° (Figure 2).

The trifluoromethanesulfonate anions are poorly defined by the data; their distances and angles are listed in Table SIV (supplementary material). The acetone molecules are somewhat better behaved in that the C—C and C=O distances are reasonable, but the thermal parameters of all eight acetone atoms are large (B's of 11–14 $Å^2$), suggesting some disorder in the region. As a consequence of these problems, all bond distances and angles in the structure have esd's larger than normal, although the geometry of the osmium–pyrene fragment appears satisfactory.

Cyclic Voltammetry. A study of the cyclovoltammetric behavior of both the mononuclear and binuclear complexes in acetone solution at room temperature was made. In Figure 3, a trace for the mononuclear complex is shown. The signal at $E_{1/2}$ = 0.52 V can be assigned the 3+/2+ couple for the complex itself; that at −0.19 V, to $[Os(NH_3)_5(N{\equiv}CPh)]^{3+/2+}$, introduced as an internal standard. The two waves, E_{pc} at −0.38 and −0.65 V, correspond respectively to the reduction of the acetone and triflate complexes of Os(III) which result on the release of Os(III) from pyrene.[7b] The half-time for this process is estimated to be several seconds. Figure 4 shows two cyclic voltammograms of **2**, in acetone as a solvent. In the case of the upper trace, the oxidation sweep was carried far enough to reveal two waves (E_{pa} = 0.72 and 0.62 V), which we assign to the stages 4+ → 5+ and 5+ → 6+ of the binuclear species. A single complementary reduction wave is observed, E_{pc} = 0.53 V, of considerably lower amplitude than the combined oxidation waves. When scanning proceeds to more negative potentials, substantial signals are revealed corresponding to the reduction of the acetone and triflate complexes, thus showing that Os(III) has been liberated in passing through

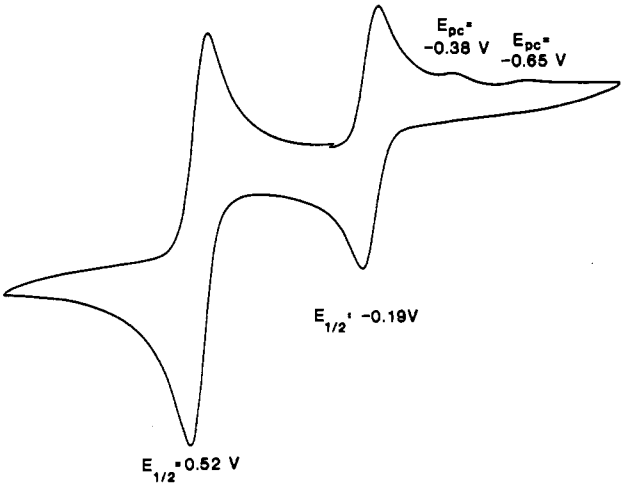

Figure 3. Cyclic voltammogram for the mononuclear complex. Conditions: concentration, 10 mM in acetone; supporting electrolyte, 0.50 M NaOTf; room temperature; sweep rate, 100 mV s^{-1}.

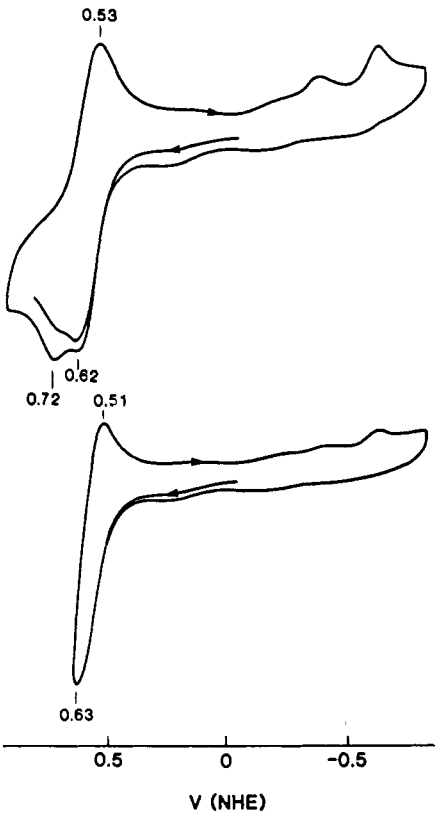

Figure 4. Cyclic voltammograms for the binuclear complex. Conditions: concentration, 10 mM in acetone; supporting electrolyte, 2 M TBAH; room temperature; sweep rate, 100 mV s^{-1}. In the experiment for the lower trace, the oxidation sweep was carried just past the first oxidation wave.

the oxidation waves. There is also a weak signal for a reversible couple at −0.20 V, which appears in variable strength in different runs and which we attribute to an impurity. In the lower trace, the oxidation sweep was carried just past the first wave so that mainly only the mixed-valence molecule forms. There appears to be no great change in the fraction of the Os(III) that is released from the organic ligand, compared to that which occurs in generating the fully oxidized species, and there is no reason to believe that there is much kinetic stabilization of the mixed-valence compared to the fully oxidized form. For both, $t_{1/2}$ for loss of Os(III) appears to be somewhat smaller than for the mononuclear complex.

The high lability of the mixed-valence state is suggested also by an experiment in which the scan rate was decreased by a factor

10. The two oxidation peaks were found to coalesce to a single broader wave, at $E_{pa} = 0.63$ V. It appears that at this slow scan rate the mixed-valence species does not survive long enough to be oxidized to the 6+ state (it should be noted that 0.63 V exceeds E_{pa} for the mononuclear species (0.52 V)).

The general features are preserved when the solution is diluted by a factor of 10, and we conclude that the mixed-valence form disappears by release of Os(III) rather than by disproportionation, which is the result expected if the labilities to loss of Os(III) are not much different for the fully oxidized acid and half-oxidized species. The dilution experiment sets an upper limit of ca. 1×10^6 M^{-1} s^{-1} on the specific rate for electron transfer, which is in line with estimates of the rates of self-exchange for couples of the type $[Ru(NH_3)_5L]^{3+/2+}$, where L is a π-acid ligand.

Discussion

In the major resonance forms for pyrene, the double bond is retained in the C1–C8 positions (the numbering scheme followed in the discussion is that indicated in Figure 1). In harmony with this, the C1–C8 bond distance is the shortest observed in the free ligand, and Hückel calculations[8] yield the highest bond orders for C1–C8. The results of new calculations[9] show that binding across the C1 and C8 positions offers the maximum overlap with the osmium d_{xz} (or d_{yz}) orbital, the corresponding coefficients of the LUMO being largest in absolute value and opposite in sign, thus providing for effective back-donation from the osmium to the pyrene. In addition, across C1 and C8 the HOMO has coefficients that are large and have the same sign, thus providing for effective σ donation from ligand to metal. Finally, we note that attachment of the first $Os(NH_3)_5$ to the C1–C8 positions does not interrupt the "aromatic" stabilization of the laterally joined rings, nor does the second, and the structure observed for the binuclear ion conforms to expectation based on these considerations.

The C1–C8 bond (1.44 Å) is significantly (0.08 Å) longer than that in the parent pyrene (1.36 Å).[10] The longer bonds indicate σ donation from the pyrene to the osmium atoms and back-donation from them to the pyrene π^* orbital. The longer C1–C2 (or C1–C8) bond (by 0.05 Å) is in line with disruption of conjugation in this ring. Also, the angle between the pyrene plane and the Os–C1–C8 plane (105 (4)°) indicates that C1 (C1′) and C8 (C8′) have fairly strong sp^3 character.

In Table III, the N1–Os–N3 angle can be read as 162.1 (5)°, far from the 180° expected if there were no distortion, and thus suggesting significant nonbonding repulsion between the cis NH_3 and the pyrene ring.

In contrast to $[Os(NH_3)_5(C_6H_6)]^{2+}$, which is fluxional on the NMR time scale at room temperature,[2a] the mononuclear pyrene complex assumes a fixed position. This is hardly surprising because, in line with arguments already introduced, relocation to one of the laterally joined rings would result in a much less stable rearrangement. The mononuclear complexes with naphthalene and anthracene also assume fixed configurations at room temperature, movement between equivalent positions on the same ring, let alone movement to another, being slow on the NMR time scale.

The electrochemical results for the pyrene binuclear complex show that the coupling between the two sites is weak. The stabilization of the mixed-valence form with respect to the isovalent forms is reflected in the value of the comproportionation constant, which, as calculated from the difference in the potentials for the two states of oxidation, is only 50. Because the separate waves do not measure equilibrium potentials, the quotient cited is to be taken as approximate, but the equilibrium value is unlikely to be higher than 1×10^2, and a value even larger can result from purely electrostatic effects.[11] That the electronic coupling is weak is not unexpected, in view of the known weaker coupling between metal ions interacting through carbons situated mutually meta.[12] It should be noted that no bond path in pyrene provides for conjugation between the two positions in question. By way of contrast, the electronic coupling in the mixed-valence form of the binuclear benzene adduct appears to be very strong. The comproportionation constant as calculated from the electrochemical results[2a] is 2.5×10^8; this high value and the nature of the absorption in the near-IR region show that face-to-face coupling by benzene leads to a valence-delocalized structure.

The cyclic voltammetry results show that the mixed-valence molecule has a very short half-life—$t_{1/2} \sim 1$ s at room temperature—so short as to make a recording of the near-IR spectrum difficult. The short half-life compared to that of $[(Os(NH_3)_5)_2(C_6H_6)]^{5+}$ ($t_{1/2} > 1/2$ h) is in line with the arguments which have already been advanced, namely that the latter mixed-valence species is greatly stabilized by electron delocalization. Also significant is the comparison of the lability of η^2 Os(III) bond compared to that observed for ethylene. The complex $[\eta^2\text{-}Os(NH_3)_5(C_2H_4)]^{3+}$ is stable for many hours in solution[2a] while $Os(NH_3)_5^{3+}$ is lost from the mononuclear pyrene complex on the time scale of several seconds and from the binuclear on the time scale of about 1 s. Significant conjugation of the C1–C8 bond with other multiple bonds in the molecule, and possibly steric effects as well, contribute to this lability.

Acknowledgment. Support of this work by National Institutes of Health Grant GM13638-22 is gratefully acknowledged. W.P.S. also acknowledges National Science Foundation Grant CHE-8219039 for the purchase of the diffractometer and the Exxon Educational Foundation for financial support. M.S. acknowledges support by a Fellowship from Mitsubishi Paper Mills, Ltd. Advice from and helpful discussions with Drs. W. Dean Harman, John Dobson, and Mitsuru Sano are also gratefully acknowledged.

Supplementary Material Available: Tables SI–SIV, listing crystal and intensity collection data, nonbonded contacts around Os, anisotropic displacement parameters, and complete distances and angles (5 pages); Table SV, giving observed and calculated structure factors (12 pages). Ordering information is given on any current masthead page.

(8) Berthier, G.; Caulson, C. A.; Greenwood, H. H.; Pullman, H. A. *C. R. Hebd. Seances Acad. Sci.* **1949**, *226*, 1906.
(9) The orbital coefficients were not given in ref 8, and the calculations were repeated by Mr. K. Mogi of Nagoya University, to whom we express our appreciation.
(10) Hazell, A. C.; Larsen, F. K.; Lehmann, M. S. *Acta Crystallogr.* **1972**, *B28*, 2977.
(11) Sutton, J. E.; Taube, H. *Inorg. Chem.* **1981**, *20*, 3125.
(12) Richardson, D. E.; Taube, H. *J. Am. Chem. Soc.* **1983**, *105*, 4.